



## Al Schottky contact on p-GaSe

Wen-Chang Huang<sup>a,\*</sup>, Shui-Hsiang Su<sup>b</sup>, Yu-Kuei Hsu<sup>c</sup>,  
Chih-Chia Wang<sup>d</sup>, Chen-Shiung Chang<sup>c</sup>

<sup>a</sup> Department of Electronic Engineering, Kun Shan University, No. 949, Da Wan Rd., Yung-Kang City, Tainan Hsien, 710, Taiwan, ROC

<sup>b</sup> Department of Electronic Engineering, I-Shou University, I, Section 1, Hsueh-cheng Rd., Ta-Hsu Hsiang, Kaohsiung County, 840, Taiwan, ROC

<sup>c</sup> Institute of Electro-Optical Engineering, National Chia Tung University, Hsinchu, Taiwan, ROC

<sup>d</sup> Institute of Electro-Optical Engineering, National SunYat-sen University, No. 70, Lien Hai Rd., Kaohsiung, Taiwan, ROC

Received 1 May 2006; accepted 6 July 2006

Available online 22 August 2006

---

### Abstract

A new Schottky diode, Al/p-GaSe, was presented in this study. It shows an effective barrier height of 0.96 eV with an ideality factor of 1.24 over five decades and a reverse leakage current density of  $4.12 \times 10^{-7}$  A/cm<sup>2</sup> at  $-2$  V after rapid thermal annealing at 400 °C for 30 s. The generation–recombination effect of the Schottky diode was decreased as the annealing temperature was increased. The formation of Al<sub>1.33</sub>Se<sub>2</sub> was observed by X-ray diffraction analysis after the diode was annealed at 400 °C for 30 s. Owing to the grains' growth, the surface morphology of the 400 °C-annealed diode was rougher than that of the unannealed diode, which was observed both by the AFM and the SEM analysis.

© 2006 Elsevier Ltd. All rights reserved.

*Keywords:* GaSe; Schottky contact; Barrier height

---

### 1. Introduction

Layered III–VI semiconductors, among them gallium selenide (GaSe), are known to present outstanding nonlinear optical properties which have been widely investigated during the last few years. Their refractive index anisotropy makes them suitable for second harmonic generation [1],

---

\* Corresponding author. Tel.: +886 6 2050521.

E-mail address: [wchuang@mail.ksu.edu.tw](mailto:wchuang@mail.ksu.edu.tw) (W.-C. Huang).

parametric oscillation [2], and frequency mixing [3] in the middle infrared spectral zone where they are transparent.

GaSe is a native p-type semiconductor, while the electrical and optical characteristics of GaSe crystal material when doped with elements in groups I, II, IV, and VII had been reported. Hole concentrations of the order of  $10^{15}$ – $10^{16}$   $\text{cm}^{-3}$  at room temperature have been obtained by doping with Cd, Zn, Cu, and Ag. The electrical and material characteristics with a hole concentration of about  $1.5 \times 10^{17}$ – $6 \times 10^{17}$   $\text{cm}^{-3}$  when doped by Er have been reported in our previous study [4]. Gallium selenide has a relatively large band gap energy of 2.0 eV, so it has potential applications to photoelectric devices that operate in the visible region [5]. Device applications such as the GaSe/GaSe<sub>1-x</sub>S<sub>x</sub> multi-quantum well structure [6] have been used to realize visible light emitter diodes. The gallium selenide crystal was also used as the material for nuclear particle detectors [7]. The detector was constructed using a scheme, Ag/GaSe/Sn, to evaluate the average energy needed to produce an electron–hole pair through nuclear particles. In order to attain devices such as light emitter diodes or nuclear particle detectors with acceptable characteristics, high quality metal contacts to GaSe are necessary. While the reports relating metal contacts to GaSe were very few. Hughes et al. [8] discussed the Fermi level un-pinning effect of the metal contact to GaSe. Gozzo et al. [9] studied the material characteristics of gold contact to GaSe, but with a lack of electrical characteristics. In the research, both the electrical and material characteristics of the Schottky diode, Al/p-GaSe, were studied. The p-type gallium selenide crystal was doped with Er, and its hole concentration is about  $1.53 \times 10^{17}$   $\text{cm}^{-3}$ . The metal electrode was evaporated through evaporation. The current–voltage characteristic was measured by a semiconductor parameter analyzer. The material characteristic of the diode was evaluated by X-ray diffraction analysis (XRD), scanning electron microscopy (SEM) and atomic force microscopy (AFM).

## 2. Experiment

The p-type Er:GaSe crystals used in this study were obtained by the Bridgmann method. Er with a purity of 99.95% was added to a stoichiometric melt of GaSe. Raw materials were enclosed in a well-cleaned quartz tube at  $10^{-6}$  Torr. Growth proceeded with a thermal gradient of 30 °C/cm and a growth rate of 2 cm/day. After growth, square samples with faces perpendicular to the *c* axis were prepared using a razor blade; their typical dimensions were  $4 \times 4 \times 0.3$  mm<sup>3</sup>. The Hall coefficients were found using a four-point direct current Van Der Pauw configuration at temperatures between 80 and 300 K to obtain the effects on the concentration and mobility of carriers. The current was made to flow in the surface planes and a magnetic field (~0.5 T) was applied perpendicular to these planes. The carrier concentration of the GaSe:Er crystal is  $1.53 \times 10^{17}$   $\text{cm}^{-3}$  and resistivity is 1.199  $\Omega$  cm. A thermal evaporator was used to deposit aluminum on the front surface of GaSe substrate in a vacuum of  $1 \times 10^{-6}$  Torr. The shadow mask was used to define the pattern of the aluminum metal electrode. The thickness of the aluminum is 100 nm, and the Schottky contact electrodes were circles with diameters of 200  $\mu\text{m}$ , 300  $\mu\text{m}$  and 400  $\mu\text{m}$  respectively. After metal deposition, the samples were treated by rapid thermal annealing (RTA) at 200 °C, 300 °C and 400 °C, respectively for 30 s. The ohmic contact on the back side of GaSe substrate was then formed by soldering high-purity indium. The current–voltage (*I*–*V*) characteristic was measured at room temperature by using an HP-4145B semiconductor parameter analyzer. The rectified characteristics, including Schottky barrier height, ideality factor and reverse leakage current, were evaluated. The XRD was used to identify the variation of

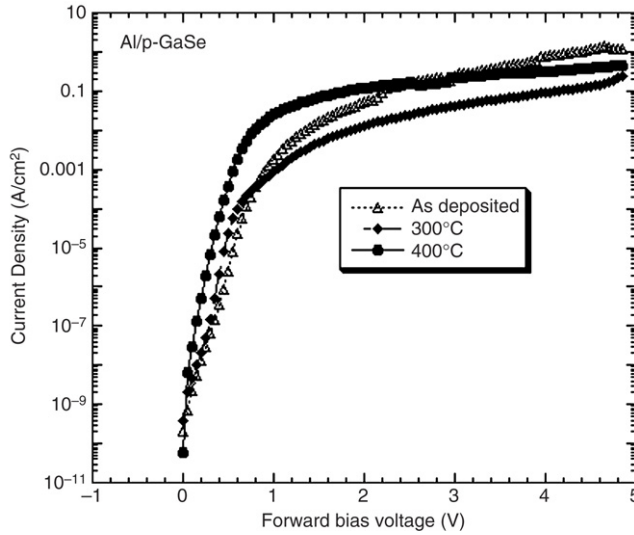


Fig. 1. The forward bias  $I$ - $V$  characteristic of the Al/p-GaSe diodes as a function of annealed temperature.

phases after the diode was treated at different annealing temperatures. Both SEM and AFM were used to observe the surface morphology of the diodes.

### 3. Results and discussion

The effective barrier height  $\phi_b$  and ideality factor  $n$ , were determined by using the thermionic emission current voltage expression:

$$I = I_s \left[ \exp \left( \frac{q(V - IR_s)}{nkT} \right) - 1 \right] \quad (1)$$

$$\text{where } I_s = AA^{**}T^2 \exp[-q\phi_b/kT] \quad (2)$$

where  $R_s$  is the series resistance of the diode,  $V$  is the applied voltage,  $q$  is the electronic charge,  $k$  is the Boltzmann constant,  $T$  is the absolute temperature,  $A$  is the diode contact area,  $A^{**}$  is the effective Richardson constant,  $\phi_b$  is the effective Schottky barrier height (SBH) at zero bias, and  $n$  is the ideality factor. A theoretical  $A^{**}$  value of  $247 \text{ A cm}^{-2} \text{ K}^{-2}$  was used for GaSe. The value is based on effective electron mass using  $m_n = 0.5m_0$ . The ideality factor is derived from  $n = q/kT[\partial V/\partial(\ln J)]$ .

Fig. 1 shows the forward characteristics of the Al/p-GaSe contact. The saturation current density,  $J_s$ , is  $4 \times 10^{-10} \text{ A/cm}^2$  for the as-deposited contact,  $7 \times 10^{-10} \text{ A/cm}^2$  for the  $300^\circ\text{C}$  annealed contact and  $2 \times 10^{-9} \text{ A/cm}^2$  for the  $400^\circ\text{C}$  annealed contact. Their effective Schottky barrier height is 0.99 eV, 0.98 eV and 0.96 eV for the as-deposited,  $300^\circ\text{C}$ -annealed, and  $400^\circ\text{C}$ -annealed contacts, respectively. The formation of the barrier arose from when the metal was in contact to GaSe: electrons flow from the metal into the semiconductor till the Fermi levels on the two sides are aligned. These electrons are minority carriers in the p-type GaSe. After reaching the semiconductor they recombine with holes giving rise to a space charge layer of ionized acceptor layer. The space charge region yielded a diffusion barrier at the contact interface. The ideality factor of the as-deposited contact is 2.1, of the  $300^\circ\text{C}$ -annealed contact is 1.84 and of

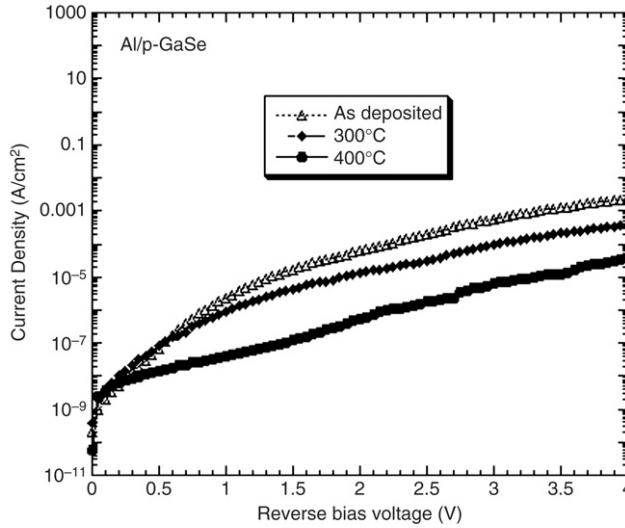


Fig. 2. The reverse bias  $I$ – $V$  characteristic of the Al/p-GaSe diodes as a function of annealed temperature.

the 400 °C-annealed contact is 1.24. The ideality factor revealed that the as-deposited contact shows recombination effect during forward bias. As the annealing temperature was increased, the ideality factor moved closer to 1. This indicates that the surface states were passivated and generation–recombination effects were decreased after the thermal annealing.

For the reverse bias current–voltage characteristics, due to the presence of image-force induced barrier lowering, the reverse current can be expressed from Eq. (1) as

$$I_R = AA^{**}T^2 \exp\left[\frac{q}{kT}(\phi_b - \Delta\phi_b)\right] \tag{3}$$

where  $\Delta\phi_b$  is the image-force barrier lowering given by  $\sqrt{qE_m/4\pi\epsilon}$ , where  $E_m$  is the maximum electric field strength at the contact and  $\epsilon$  is the GaSe permittivity. The reverse current shown in Fig. 2 is several orders of magnitude higher than expected values from Eq. (3) and indicates the mechanisms such as surface leakage, depletion layer generation or defect-assisted tunneling are present. Fig. 2 shows the reverse characteristics of the Al/p-GaSe contacts after different annealing temperatures. The reverse leakage current depends on both bias and annealed temperature. As the reverse bias voltage increased the leakage current increased, while the leakage current could be reduced as it was passed through thermal annealing. The reverse leakage current density is equal to  $5.73 \times 10^{-4}$  A/cm<sup>2</sup> at the bias of 3 V of the as-deposited diode. It could be improved to  $9.28 \times 10^{-5}$  A/cm<sup>2</sup> as it was treated with 300 °C annealing for 30 s. Also, it could be further improved to  $6.4 \times 10^{-6}$  A/cm<sup>2</sup> as the annealing temperature was increased to 400 °C. This result accounts for the passivation of defects or interface states of the contact interface after thermal annealing.

Fig. 3(a) shows the XRD analysis of the as-deposited Al/p-GaSe diode. Most of the diffraction peaks belong to the phases of GaSe. The diffraction angles of GaSe(004) were centered at  $2\theta = 22.16^\circ$ , of GaSe(006) were centered at  $2\theta = 33.58^\circ$ , of GaSe(1010) were centered at  $2\theta = 39.42^\circ$ , of GaSe(008) were centered at  $2\theta = 45.34^\circ$ , and of GaSe(0010) were centered at  $2\theta = 57.62^\circ$ . The diffraction peak of Al(111) was that corresponding to  $2\theta = 38.58^\circ$ . As the

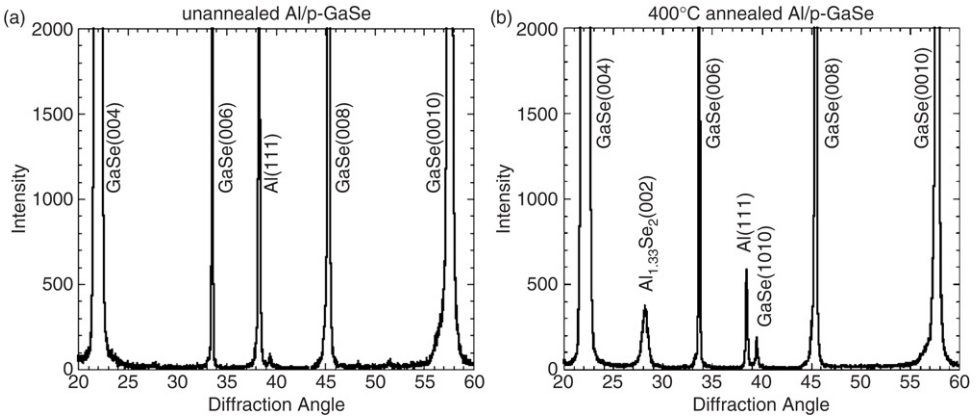


Fig. 3. The XRD spectrum of Al/p-GaSe diodes (a) as deposited, (b) after RTA at 400 °C for 30 s.

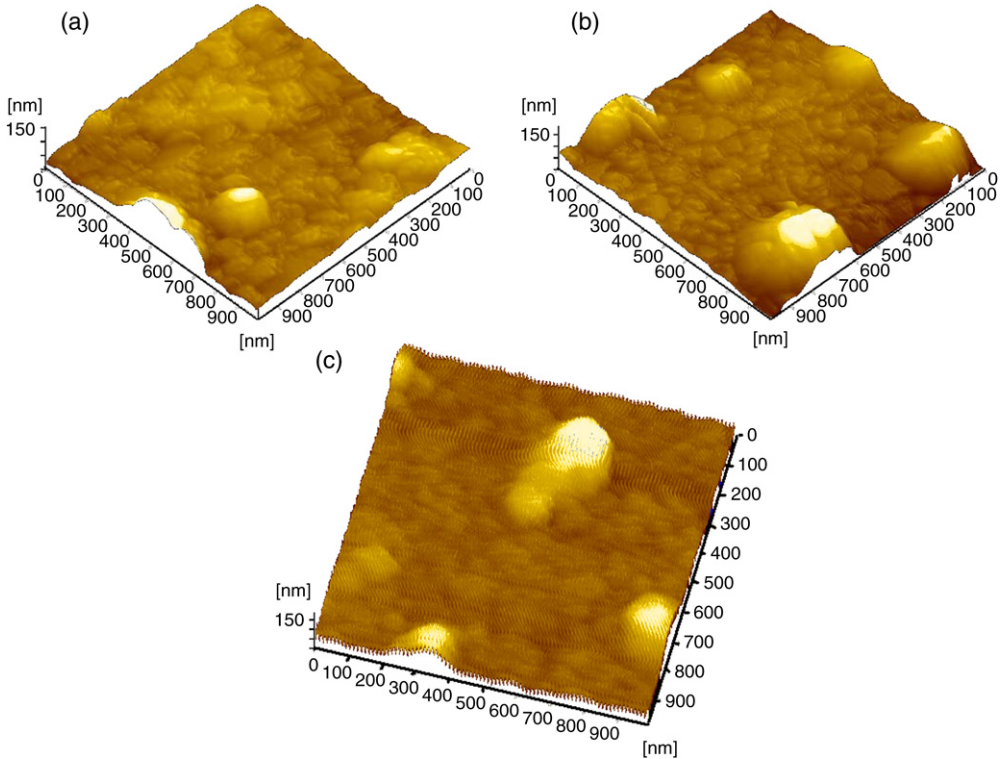


Fig. 4. The AFM pictures of Al/p-GaSe diodes (a) as deposited, (b) after RTA at 300 °C for 30 s, (c) after RTA at 400 °C for 30 s.

diode was treated with RTA annealing at 400 °C for 30 s, a new phase of Al<sub>1.33</sub>Se<sub>2</sub> was found at  $2\theta = 28.3^\circ$  as shown in Fig. 3(b). This means that the reaction between Al and GaSe occurred after the thermal annealing.

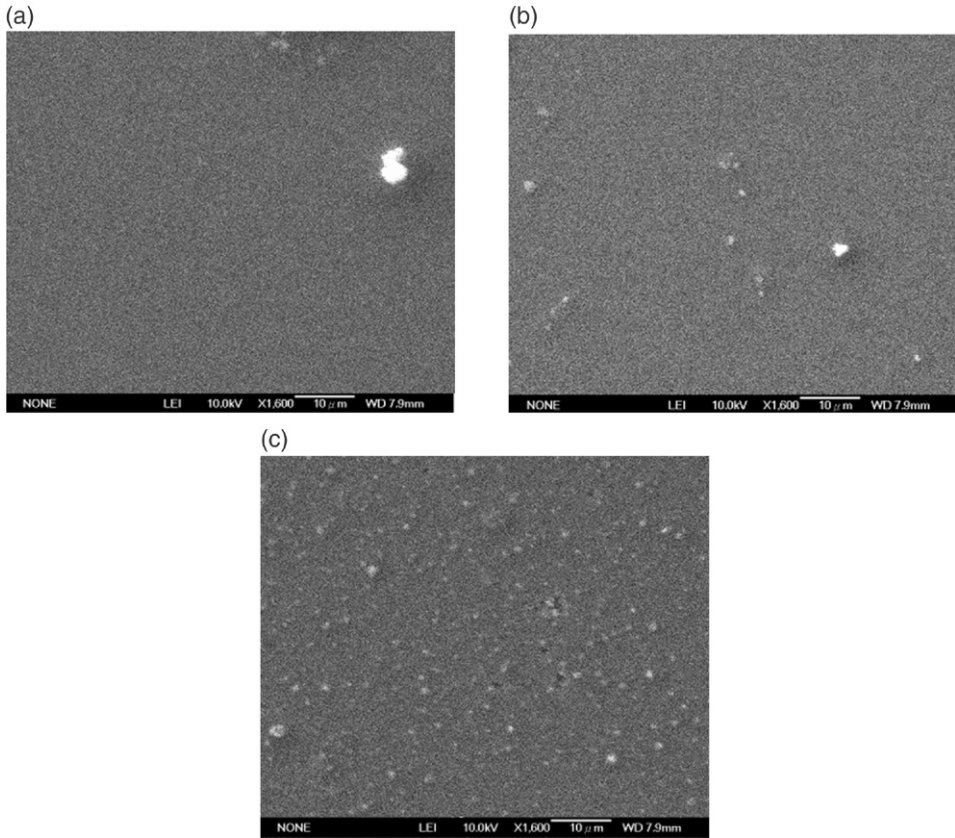


Fig. 5. The SEM pictures of Al/p-GaSe diodes (a) as deposited, (b) after RTA at 300 °C for 30 s, (c) after RTA at 400 °C for 30 s.

Fig. 4(a), (b) and (c) show the AFM pictures of the as-deposited diode, the 300 °C-annealed diode, and the 400 °C-annealed diode, respectively. The area of these diodes which were shown on the AFM pictures is  $1 \mu\text{m}^2$ . The root mean square (RMS) value is equal to 1.56, 2.74 and 2.87 for the as-deposited diode, 300 °C-annealed diode and 400 °C-annealed diode, respectively. The rough surface morphology of the 400 °C-annealed diode was due to the reaction between Al and GaSe which produced new grains and these grains lead to the roughness of the contact surface.

Fig. 5(a), (b) and (c) show the SEM pictures of the as-deposited diode, the 300 °C-annealed diode, and the 400 °C-annealed diode, respectively. Each area of the contact surface was equal to  $75 \times 55 \mu\text{m}^2$  which was shown in these SEM pictures. A very smooth surface morphology was shown at the surface of the as-deposited diode. As the annealed temperature was increased, the contact gradually showed rough surface morphology. As it was increased to the annealing temperature of 400 °C, many small bulges were observed at the surface.

The Al/p-GaSe showed better electrical characteristics after it was treated with RTA annealing. These annealings passivated the interface states of the contact interface. The generation–recombination effect of the diode which was in response to the bias voltage was degraded. It was confirmed by the observation of the ideality factor at forward bias and by the lowering of the leakage current density at reverse bias of the annealed diodes.

#### 4. Conclusion

A new Schottky diode, Al/p-GaSe was realized in this research. It showed an effective Schottky barrier height of 0.94 eV with an ideality factor of 1.24 at the 400 °C-annealed diode. The contact interface of the diode was passivated after thermal annealing. The passivation gave rise to a lower reverse leakage current and a better ideality factor. A new phase of Al<sub>1.33</sub>Se<sub>2</sub> was formed and the surface became rough after the thermal annealing.

#### Acknowledgment

The authors would like to thank the National Science Council of the Republic of China, for financially supporting the research under Contract No. NSC-94-2216-E-168-004.

#### References

- [1] E. Bringuier, A. Bourdon, N. Piccioli, A. Chevy, Phys. Rev. B 49 (1994) 16971.
- [2] K.I. Vodopyanov, L.A. Kulevskii, V.G. Voevodin, A.I. Gribenyukov, K.R. Allakhverdiev, T.A. Kerimov, Opt. Commun. 83 (1991) 322.
- [3] A. Bianchi, A. Ferrario, M. Mucsi, Opt. Commun. 25 (1978) 256.
- [4] Y.-K. Hsu, C.-S. Chang, W.-C. Huang, J. Appl. Phys. 96 (2004) 1563.
- [5] S. Shigetomi, T. Ikari, H. Nakashima, J. Appl. Phys. 74 (1993) 4125.
- [6] M. Budiman, T. Okamoto, A. Yanada, M. Konagai, Japan. J. Appl. Phys. 37 (1998) 5497.
- [7] E. Sakai, H. Nakatani, C. Tatsuyama, F. Takeda, IEEE Trans. Nucl. Sci. 35 (1988) 85.
- [8] R.H. Williams, A. Mckinley, G.J. Hughes, V. Montgomery, I.T. McGovern, J. Vac. Sci. and Technol. 21 (1982) 594.
- [9] F. Gozzo, M. Marsi, H. Berger, G. Margaritondo, A. Ottolenghi, A.K. Ray-Chaudhuri, W. Ng, S. Liang, S. Singh, J.T. Welnak, J.P. Wallace, C. Capasso, F. Cerrina, Phys. Rev. B 48 (1993) 17163.